
CONTRIBUTED PAPERS

USING THE X-RAY TUBE WHITE RADIATION SPECTRUM

J. R. HESTER

National Institute for Research in Inorganic Materials, 1-1 Namiki, Tsukuba, Ibaraki 305

Practical aspects of using white radiation from an X-ray tube are treated. Possible problems, including peak shape, polarisation effects and equipment limitations, are discussed. A brief summary of an investigation into the wavelength dependent behaviour of extinction is presented as an example of an application of the white radiation spectrum.

1. Introduction

Most single crystal X-ray diffraction experiments carried out in the laboratory are performed at the characteristic wavelength of the X-ray target in order to maximise the measured intensity. A significant amount of the energy of the electron beam incident on the target is radiated at other wavelengths ("Bremsstrahlung" or "white radiation") and can be made use of if the appropriate equipment is available. In the following discussion, the words 'energy' and "wavelength" are used interchangeably, with the understanding that they are inversely proportional to one another. A more detailed discussion on energy dispersive methods than that given in this article can be found in [1] and [2].

2. Background

2.1. Experimental Arrangement

A normal four-circle single crystal diffractometer is the basis for the experimental arrangement used below. There is no monochromator, and the detector scintillator crystal and photomultiplier are replaced by a solid-state detector (SSD), which outputs a voltage pulse with amplitude proportional to the energy of the incident photon. Such a detector is normally unable to resolve the peak splitting between α_1 and α_2 lines, giving it little advantage over a monochromator. However, it can resolve this splitting when a W target is used, making a monochromator unnecessary.

The voltage signal is passed to a discriminator, either single channel (SCA) or multiple-channel (MCA). Multiple-channel analysers are convenient for rapid investigation of the entire reflected spectrum; however, computer-controlled measurement of broad regions in energy is limited by the time required

to transfer the MCA data to the computer, typically of the order of 1/100 s per channel.

The experimental configuration in our laboratory is illustrated in figure 1. A Rigaku-built, horizontally mounted X-ray tube operating at 150 kV and 12 mA produces electrons which strike a W target, emitting X-rays with characteristic wavelength 0.20899 Å ($K\alpha_1$). These X-rays are diffracted by the sample into a solid Ge detector. Voltage pulses from this detector are preamplified and passed to a MCA. The MCA is under direct computer control through a GPIB interface. Further details are given in [3].

2.2 Peak Shape and Limits

The peak shape normally observed is dominated by the convolution of contributions due to (a) mosaic distribution (b) source size and (c) spectral distribution [4]. For all reflections measured at a given wavelength to be directly comparable, the measured profiles should be produced at the same incident intensity of the same wavelength spectrum. Thus, in an experiment with monochromator and scintillator crystal detector, $\omega/2\theta$ detector scans are used and the width of the scans varied so that reflected photons originating from the same incident wavelength band are measured. The reason for this appears to be that total scanning time is reduced, as scan width can be expanded in proportion to the width of the $K\alpha$ doublet, rather than set at the maximum observed value. ω scans are also viable, providing that the entire 2θ distribution for each reflection is incident on the aperture at all ω and 2θ settings of interest.

When using a SSD, the wavelength cutoff is sharp, and a smaller wavelength band can be chosen than that used in conventional experiments. As a con-

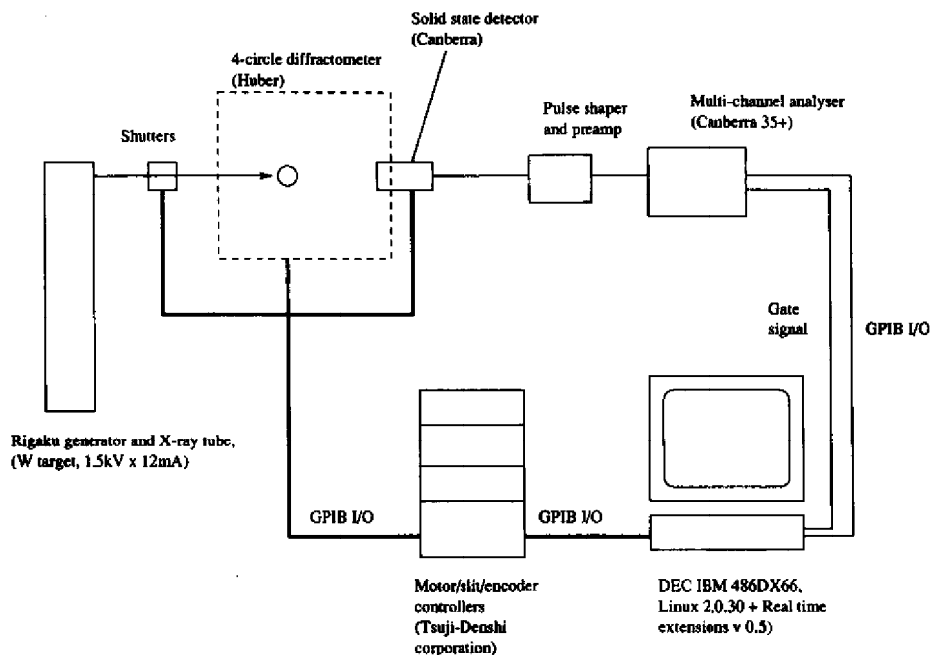


Fig. 1 Equipment configuration for experiments using white radiation from an X-ray tube.

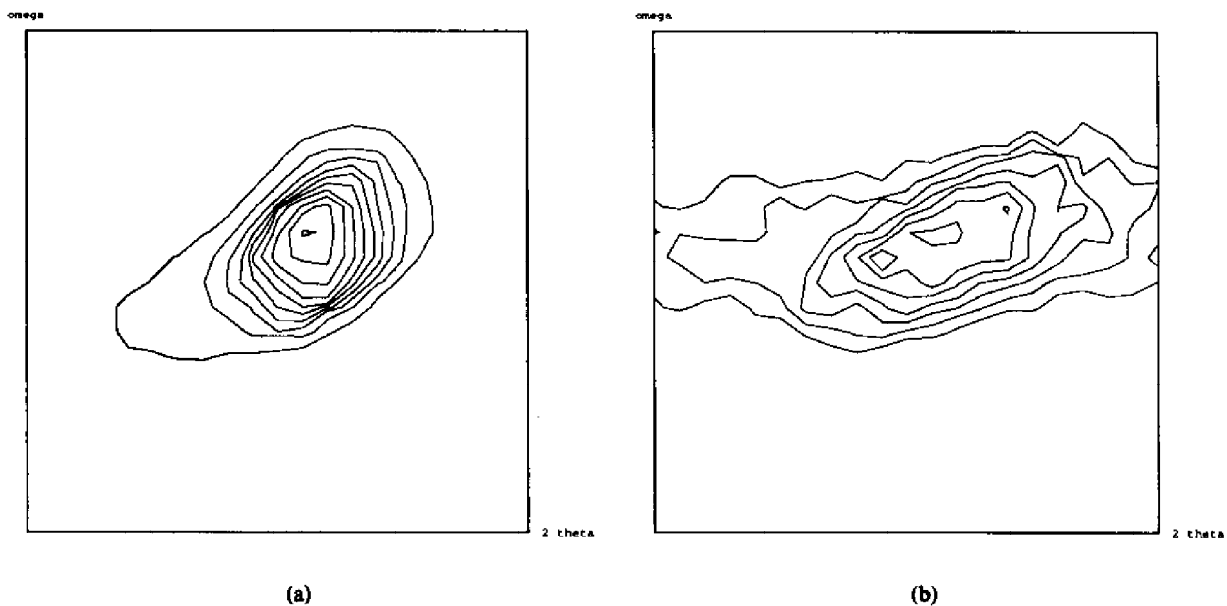


Fig. 2 $\omega, 2\theta$ plots of the ZnO 105 reflection using (a) tungsten $K\alpha_1$ radiation (b) 0.15 Å radiation from the same source. Plots were produced by scanning the 2θ axis at fixed ω for each ω setting using a 0.3 mm slit. Ω axis is vertical, 2θ horizontal. Borders 0.4° . Elongation in the 2θ direction in (b) is due to partial transmission of the high-energy photons through the slit walls.

sequence, the variation in the angular width of the peaks due to the wavelength spectrum is much smaller. There is therefore little advantage in using a variable scan width, so $\omega/2\theta$ scans are replaced by fixed-width ω scans.

While the wavelength range is easily chosen when using the $K\alpha_1$ line by finding the boundaries of the peak in a plot of intensity versus wavelength, it is not so obvious what energy window should be chosen when using white radiation. After consideration of the above discussion, it should be clear that any range is acceptable, provided that the scan width and aperture are chosen such that all photons in that range will enter the aperture at some point in the scan. The width in energy is also limited by the assumption that all angular and wavelength-dependent effects, e.g. Lorenz and polarisation corrections, are effectively constant over the width of the peak.

To illustrate the points made above, some representative two-dimensional $\omega:2\theta$ scans are shown in Fig 2. Scans were performed using the method described by [4]: a narrow aperture (0.3 mm) was used and the 2θ range scanned at fixed ω . Repeating this procedure for all ω produces a diagram of the peak which is useful for interpretation. Projection of the peak intensity onto the ω axis in our diagram produces a normal, one-dimensional ω scan, where the peak shape is largely determined by the mosaic distribution. The contribution of wavelength dispersion lies along a 45° line in the diagram. Suitable re-plotting of the data, so that the $\omega/2\theta$ axis is vertical, would allow similar recreation through horizontal projection of a one-dimensional $\omega/2\theta$ scan.

As can be seen from Fig. 2, peak shapes from white radiation do not differ fundamentally from those normally seen in ordinary work.

2.3 Polarisation

The polarisation of the X-ray beam produced by an X-ray tube varies with energy [5]. Polarisation is defined as

$$P(E) = [i_n(E) - i_p(E)]/[i_n(E) + i_p(E)]$$

where i is the intensity and the subscripts refer to the normal and parallel polarisation components relative to the plane defined by the electron beam and the X-rays incident on the sample. For purposes of comparison of different targets, the energy is expressed as

a proportion of the energy of the electrons incident on the target (T).

At operating energies for which $E/T < 0.7$, P is of the order of -0.05 – -0.1 [5], that is, photons tend to be slightly polarised parallel to the reflection plane. Above $E/T = 0.8$, P begins to drop, so that $P(0.9)$ is ≈ -0.3 . Polarisation approaches -1.0 as E/T approaches 1.

The measured intensity for a given hkl can be expressed as

$$IH = k \times d^2 |F| i_o(E) C_{pH}$$

Here d is the lattice spacing, F is the structure factor, i_o is the incident beam intensity, and C_p is the polarisation factor. The subscript H refers to the given hkl.

The polarisation factor, C_p , is a function of E and θ , the diffraction angle (we have assumed here, for simplicity, that the electron beam and emitted X-ray are at 90° to one another):

$$C_p = \frac{1}{2} [1 + |\cos 2\theta| + P(E)(1 - \cos 2\theta)]$$

Thus, for small 2θ , the effect of changing $P(E)$ is virtually negligible. For example, if $2\theta = 10$, the difference between $P(E) = 0$ and $P(E) = -0.3$ is only 0.5%. The difference is significant at large angles and large E/T , which are not normally used. So for $2\theta = 70$, the error in assuming that $P(E)$ is zero is about 5% for a typical tube with $E/T < 0.7$, and grows to 10% if $E/T = 0.9$.

The user of white radiation should therefore be aware that near the higher limit of tube energies they may need to use a different polarisation ratio to that used when measuring at the characteristic tube wavelength. Failure to use the proper polarisation ratio will lead to ratios of reflections collected at a single wavelength not accurately mirroring ratios of F values.

2.4 MCA Deadtime Correction

Use of a multi-channel analyser can complicate deadtime correction. A deadtime calculation based on counts seen at a particular wavelength assumes that reflected energy at other wavelengths is negligible. An obvious problem with this assumption occurs when harmonics of the target reflection are strong. In this case counts collected in other portions of the spectrum will contribute significantly to

Table 1 Experimental details for Si data collection.

Wavelength (Å)	0.25	0.209 (WK α_1)	0.184 (WK β_1)	0.15	0.11
Scan speed (°/min)	1	6	6	1	1
Total reflections	411	2355	1952	824	295
hkl range	0≤h≤8, -8≤k, l≤8	-12≤h, k, l≤12	-12≤h, k≤12, 0≤l≤12	-8≤h, k, l≤8	-8≤h≤0, 0≤k, l≤8
Max sin θ // λ (Å ⁻¹)	0.86	1.24	1.91	0.86	0.78
Instability factor	n/a	1.1x10 ⁻³	1.2x10 ⁻⁴	n/a	n/a
μ (cm ⁻¹)	0.424	0.314	0.257	0.211	0.165
Absorption Max/Min	1.18/1.14	1.13/1.10	1.11/1.08	1.09/1.07	1.07/1.05
R _{merge} (I)(%)	4.6	4.6	5.3	3.7	5.0
Independent reflections	33	82	127	33	26
Scale (F ²)	0.4185(9)	1.000(2)	2.340(8)	2.308(7)	15.2(2)
R (scale)	0.38	0.43	1.28	0.79	2.75
R	1.0	1.2	3.3	1.5	4.0
wR	0.5	0.9	1.3	1.4	1.5
S	1.2(2)	1.3(1)	1.24(8)	3.7(5)	1.9(2)
γ_{min}	0.71	0.79	0.78	0.83	0.95

deadtime. This could be solved by always reading the entire spectrum into the computer during data collection; however, this is in practice prohibitively expensive in time. For example, in our current experimental configuration using the MCA (Fig. 1) reading all 1024 MCA channels takes about 30 seconds. This is impractical in a situation where it may cause data collection time to increase by a factor of two.

Some MCAs offer hardware deadtime correction. The model used in our laboratory performs this by accumulating the time that the counter is 'dead', and then extending the counting time by that amount of time at the end of the requested time period. One disadvantage of this approach is that it restricts counting periods to multiples of those allowed by the MCA. Thus rapid step scans, where one step may involve counting for less than one second, are not possible if deadtime correction is desired, as the MCA counts time in one second units.

Furthermore, if the count rate is constantly changing, as it is during a continuous peak scan, the above-described hardware-based strategy will not work, as the extra time is added on at the end of the scan, by which time either the detector arm has finished

scanning, or only background counts are being measured. The largest count loss in the region of the peak maximum is therefore not compensated for. MCA hardware-based deadtime correction should therefore ideally involve step-scanning for time periods that are compatible with the hardware deadtime correction routine.

2.5 Other Considerations

White radiation is not normally used because it is much less intense than the K α lines. For example, a reflection collected at 0.11 Å is approximately 1000 times weaker than one collected at 0.209 Å for the tungsten tube operating at 150 kV. This difference in intensity can be partially compensated for by reducing the scan speed, but it is rarely practical to slow scanning enough to obtain data of similar accuracy. The experimenter should thus carefully weigh the gain in accuracy from slower scan speeds with the increase in time required.

The fact that white radiation is incident on the sample, rather than monochromatised radiation, might be expected to change the extinction behaviour due to interactions between photons of different energies within the crystal. However, such effects have been shown to be negligible [6].

The maximum total count rate over all channels which can reliably be recorded using a solid state detector is limited by physical effects and pile-up of the output pulses to the order of 10,000 cps. This restriction is not severe when relatively weak white radiation is used; however, if the same experimental configuration will be used for data collections carried out at the characteristic tube wavelength, it may reduce the statistical accuracy of the data obtained.

3. Example Application

In this section we describe one straight forward application of open-tube radiation. More details are available in [7]. Another application, X-ray fluorescence spectroscopy, has been described by [8] in a previous issue of this journal.

3.1 Extinction Measurement

A long-standing problem in accurate X-ray diffraction studies is that of correcting for extinction. As pointed out by [9], extinction tends to zero as the reflected intensity tends to zero. While we obviously cannot measure anything at the zero condition, we may be able to extrapolate from measurements taken sufficiently close to that condition.

Wavelength is one parameter that we can use to extrapolate against, as it fulfills the condition of zero reflection intensity at zero wavelength. As a first approximation, linear extrapolation of measurements taken at different wavelengths can be used to estimate the extinction-free intensity.

Data were collected at five wavelengths (0.11 Å, 0.15 Å, 0.184 Å, 0.209 Å, and 0.25v) using the experimental design described above. Scan speeds for the 0.11, 0.15 and 0.25 Å data collections were 1° min⁻¹, and for the other wavelengths 6° min⁻¹. The energy window was kept constant in each case. Complete spheres of data were collected at these wavelengths from a Si single crystal, and scaled together using the algorithm of [10]. Other experimental details are presented in Table 1.

Examination of the table shows that, even at the shortest wavelength, useable data could be obtained despite the large reduction in intensity.

Once the data had been placed on the same scale, the intensity of each extinction-affected reflection was plotted against wavelength and a linear least squares fit performed to find the value at $\lambda=0$, which was taken to be the extinction-free structure factor.

This value was then compared with accurate Pendellosung values [11]. The average agreement of reflections corrected in this way with the accurate values was about 3%, worse than that of a standard least squares parameter refinement including extinction using the K α data, but better than the data before extrapolation and thus shows that worthwhile information can be obtained from the white radiation spectrum.

4. Concluding Remarks

The extra time necessary to collect useful data using white radiation is a significant disadvantage of this technique. However, the advent of easy access to synchrotron radiation is reducing the time demands on laboratory tube sources, making time on them relatively less valuable for many applications. This means that time-consuming experiments involving white radiation are relatively less expensive and thus more practical than in the past.

It is difficult to say to what extent X-ray tube white radiation will be used in the future, given that the latest generation synchrotron sources provide high intensity over a large range of energies, so that any important experiment involving variable wavelengths, such as EXAFS, is more efficiently and accurately performed at the synchrotron. It is likely that laboratory white-beam techniques will therefore be most common for preliminary and less important studies.

References

- [1] Buras, B., Olsen, J. S., Gerward, L., Selsmark, B., and Anerson, A. L., *Acta Cryst.* **A**(31), 327-333 (1975).
- [2] Fukamachi, T., Hosoya, S., and Okunuki, M., *Acta Cryst.* **A**(32), 104-109 (1976).
- [3] Okamura, F. P., *The Rigaku Journal*/Vol. 11 No. 2 (1994).
- [4] Mathieson, A. M., *Acta Cryst.* **A**(38), 378-387 (1982).
- [5] Olsen, J. S., Buras, B., Jensen, T., Alstrup, O., Gerward, L., and Selsmark, B., *Acta Cryst.* **A**(34), 84-87 (1977).
- [6] Tomoyoshi, S., Yamada, M., and Watanabe, H., *Acta Cryst.* **A**(36), 600-604 (1980).
- [7] Hester, J. R. and Okamura, F. P., *Acta Cryst.* **A**(35), 50-57 (1967).
- [8] Takahashi, Y., *The Rigaku Journal*/Vol. 13 No. 1 (1996).
- [9] Mathieson, A. M., *Acta Cryst.* **A**(35), 50-57 (1979).
- [10] Monohan, J. E., Schiffer, M., and Schiffer, J. P., *Acta Cryst.* (22), 322 (1967).
- [11] Saka, T. and Kato, N., *Acta Cryst.* **A**(42), 469-478 (1986).